Article

Template-Free Synthesis of Highly Porous Boron Nitride: Insights into Pore Network Design and Impact on Gas Sorption

Sofia Marchesini, Catriona M. McGilvery, Josh Bailey, and Camille Petit

ACS Nano, **Just Accepted Manuscript** • DOI: 10.1021/acsnano.7b04219 • Publication Date (Web): 11 Sep 2017

Template-Free Synthesis of Highly Porous Boron Nitride: Insights into Pore Network Design and Impact on Gas Sorption

Sofia Marchesini[a], *Catriona M. McGilvery*[b], *Josh Bailey*[c] *and Camille Petit*[a,]*

[a] Barrer Centre, Department of Chemical Engineering, Imperial College London, South Kensington Campus, London SW7 2AZ, UK

[b] Department of Materials, Imperial College London, South Kensington Campus, London SW7 2AZ, UK

[c] Department of Chemical Engineering, University College London, Gower Street, London WC1E 6BT, UK

*E-mail: camille.petit@imperial.ac.uk; Phone: +44 (0)20 7594 3182 (Petit C.)

ABSTRACT

Production of biocompatible and stable porous materials, *e.g.* boron nitride, exhibiting tunable and enhanced porosity is a prerequisite if they are to be employed to address challenges such as drug delivery, molecular separations or catalysis. However, there is currently very limited understanding of the formation mechanisms of porous boron nitride and the parameters controlling its porosity, which ultimately prevents exploiting the materials' full potential. Herein, we produce boron nitride with high and tunable surface area and micro/mesoporosity *via* a facile template-free method using multiple readily available N-containing precursors with different thermal decomposition patterns. The gases are gradually released, creating hierarchical pores, high surface areas (> 1900 m^2/g) and micropore volumes. We use 3D tomography techniques to reconstruct the pore structure, allowing direct visualization of the mesopore network. Additional imaging and analytical tools are employed to characterize the materials from the micro- down to the nano-scale. The CO_2 uptake of the materials rivals or surpasses those of commercial benchmarks or other boron nitride materials reported to date (up to four times higher), even after pelletizing. Overall, the approach provides a scalable route to porous boron nitride production as well as fundamental insights into the material's formation, which can be used to design a variety of boron nitride structures.

KEYWORDS: *boron nitride, adsorption, porosity, CO_2 capture, activation, TEM tomography, template-free synthesis.*

Tunable porosity and chemistry, as well as robustness, are key features of porous materials, as they are employed in a wide range of applications including gas storage, water and air treatment, industrial gas and liquid separation, drug delivery and catalysis.[1-4] Researchers have developed numerous porous materials including, but not limited to, activated carbons, zeolites, metal-organic frameworks (MOFs) and covalent organic frameworks (COFs).[5-10] A relatively recent addition to the class of porous materials is porous boron nitride (BN).[11-19] BN exhibits attractive properties such as: high chemical resistance, good thermal stability (up to 800-1000 °C in air and over 2000 °C in inert atmosphere), high thermal conductivity and mechanical resistance as well as catalytic properties.[20-26] Different allotropic forms of BN can be produced, [27] of which t-BN (turbostratic) and a-BN (amorphous) can provide the porosity desired for molecular separation and storage. Henceforth, t-BN and a-BN is referred to as porous BN. Porous BN can be obtained *via* a high-temperature reaction between a nitrogen (N)- and a boron (B)-containing precursor. This can be produced with or without the use of a solid template.[28-35] Templating also occurs as reagents release gases during their decomposition, thereby creating porosity. Such compounds are known as activating agents or structure-directing agents (*e.g.* cetyl-trimethylammonium bromide,[36] triblock copolymer P123).[37] Template-free syntheses are often preferred over template-based methods as fewer reagents and synthesis steps are required. In template-free syntheses, porous BN is typically produced from the reaction between B- and N-containing precursors at high temperatures (~1000 ºC) under an inert or ammonia atmosphere.[11,12, 14-16, 38]

The stability and potentially high porosity of BN have prompted several studies on its synthesis and subsequent application in molecular separation processes. Despite these current research efforts, our ability to tune the material's porosity and chemistry is limited, particularly *via* a cost-effective and straightforward approach. This aspect is important for ensuring the versatility of

porous BN and its relevance to the industrial sector. Among the few studies on the topic, the work of Nag and coworkers[12] is significant, indicating that the surface area of boron nitride nanosheets (BNNSs) can be increased by increasing the molar ratio of urea to boric acid. However, the porosity reported remained limited (S_{BET} < 1000 m^2/g). Wu *et al.*[39] recently obtained BNNSs with varying surface areas depending on the solvents used during the dissolution step of the precursors, prior to the synthesis of BN. Large surface areas were obtained but required a large excess of the N-containing precursor. The importance of the preparation of the intermediates of reaction was also demonstrated but the approach required long drying times.[40]

Herein, we have developed a template-free method to produce BN with tunable surface area and micro/mesoporosity using readily available chemicals. This approach relies on the use of multiple N-containing precursors and does not require any washing step (Scheme 1). With this method, a greater understanding of the formation of porous boron nitride is reached. During decomposition, the various N-containing precursors release gases, *i.e.* porogens, over a wide range of temperatures. Since the precursors only contain N, C, O and H atoms, which are either released in the form of gases or become part of the BN structure, there is no need for an extra cleaning/washing step. Depending on the conditions used, BN with very high surface area and pore volume can be produced. All samples were characterized extensively to provide insight into the chemistry, structure, porosity and morphology of BN. Scanning transmission electron microscopy (STEM) tomography was employed to directly visualize the structure of porous BN. Additional analytical tools were used to investigate the macro- to nanoporosity (*i.e.* pore location, shape, connectivity) and to understand the mechanisms of BN formation. Owing to their large micropore volume, the samples were tested for gas adsorption (CO_2, CH_4) at low (<1

bar) and high pressures (up to 20 bar). The tested BN rivals common adsorbents performance while exhibiting greater resistance to oxidation and moisture. Finally, BN pellets were produced by compression of powder samples. Minimal decreases in porosity and gas uptake were observed, which demonstrate the robustness and processability of the material, two of the requirements for application at scale. Overall, we claim that the current study brings practical insights on the synthesis of porous BN, while providing fundamental knowledge on its formation that will serve as a basis for the design of other BN structures.

RESULTS and DISCUSSION

The porous BN samples were fabricated *via* two non-templating methods (**Scheme 1**). Depending on the method, boric acid was mixed with either a single N-containing precursor or two N-containing precursors. In the former case, the samples are called "single N-precursor BN", and in the latter "multiple N-precursor BN" (Details on the naming system for the various samples can be found in Scheme 1).

In-depth characterisation of the morphology, as well as the textural features (including the pore structure and connectivity) of the synthesised samples, was performed from the micro- down to the nano-scale. XRD confirms the formation of a-BN and/or t-BN (**Fig. 1d**, **Fig. S1**). For all samples, two very broad peaks are observed at 2Theta 26° and 41° corresponding to the (002) and (100) planes of h-BN, respectively.[41] A typical spectrum for h-BN is also included for comparison (**Fig. 1b**). It is concluded that either BNNSs or a mixture of t-BN and a-BN are formed. The formation of multi-layer h-BN is excluded due to the broadness of the peaks and the absence of reflections other than (002) and (100). TEM along with fast Fourier tranform (FFT) patterns were used to determine whether BNNSs or t-BN/a-BN was formed. The sample exhibits

a disordered structure with no visible diffraction pattern (though some crystalline regions are visible, **Fig. 1c**). This is in contrast with the TEM image of BNNSs for which strong diffraction spots are observed (see **Fig. 1a**, commercial h-BN exfoliated *via* a 6-hour sonication in water). These analyses indicate the formation of amorphous porous BN.

Imaging techniques were further employed to directly visualise the morphology and pore network of the BN samples. Samples prepared using urea or biuret exhibit a flake-like morphology, similar to what would be expected for 2D nanosheets, while those prepared using melamine exhibit whisker-like morphology, with no visible macropores (**Fig. 1e-i, Fig. S2**). With increasing amounts of biuret to the urea/boric acid mixture, a transition from a flake-like morphology to a more disordered 3D network of fibers is observed (**Fig. 1i**). A disordered structure is also visible when melamine was added to a urea and boric acid mixture (**Fig. 1h**). The different features observed for the various single N-precursor samples may originate from the distinct chemical structures (**Scheme 1**) and morphologies of the precursors.[42] The larger N-precursor to B-precursor ratio used for some of the samples may have an effect as well. It is hypothesized that the addition of a second N-precursor creates 'turbulences' during the formation of BN, with more gases released over a wider temperature range. This may lead to a more disordered structure in the resulting materials.

To provide a more comprehensive view of the materials microscale features, we conducted electron tomography analyses. A single N-precursor BN was compared with a multiple N-precursor BN (**Fig. S3**). The two materials exhibit distinct morphologies, however the particles within the same material are relatively homogeneous. The single N-precursor BN has a microsponge-like structure with the presence of regular mesopores ranging from 10 to 30 nm (**Fig. 2a-c**, **Movie 1**). The pores appear spheric and their volume percentage is calculated to be

around 45 vol.%. from the 3D reconstuction. The multiple N-precursor BN exhibits smaller and inhomogeneous mesopores and appears like a crumpled nanosheet (**Fig. 2d-f**, **Movie 2**). The resolution of this technique does not allow micropores and small mesopores to be displayed.

In order to study smaller features (*i.e.* micro- and lower range mesoporosity), N_2 sorption analyses at -196 ºC were conducted (**Fig. 3**, **Fig. S4**, **Table S1**). Type IV isotherms are observed for all samples, indicating the presence of both micro- and mesopores (**Fig. 3a**, **c**). The surface area of biuret- and melamine-based samples steadily increases as more of the additional N-containing precursors is added to the system. A maximum value of 1900 m^2/g was measured, which is among the highest surface areas reported for boron nitride. For comparison, the theoretical surface area for a single atom thick sheet is ~2630 m^2/g [43]. The highest surface area for BN (2078 m^2/g) was observed by Li *et al.* for a material produced using the block copolymer P123 as a structure-directing agent.[44] However, the BN obtained in that study exhibited a large amount of impurities deriving from P123. Comparable surface area was reported by Weng *et al.*[18] using dicyanamide and boric acid precursors, which required the use of ammonia, a toxic gas, at 800 °C. The tuning of the micro/mesoporosity was not achieved in these earlier studies. A similar surface area was also measured by Wu *et al.* when using urea and boric acid in a molar ratio of 30, which were first dissolved in a methanol/water mixture.[39] The approach included an additional synthesis step as well as the use of methanol and a considerable waste of urea (which was used in large excess). In the present study, for melamine-based samples, we observe an increase in the surface area, volume of micropores and total pore volume with increasing amounts of melamine, while the mesopore volume decreases slightly. This trend suggests that increasing the amount of melamine leads to an increase in the amount of gas being released, thereby enhancing the formation of micropores. In the case of biuret-based samples, the trends

appears to be more complex than those for the melamine-based samples. Indeed, while the surface area and the micropore volume increase with increasing amount of biuret, the volume of mesopores and hence the total pore volume exhibit more uneven patterns. Adding biuret in small quantities has a detrimental effect on the mesopores. However, when the quantity of biuret is further increased, the mesopore volume increases again. This observation may be due to a combination of factors, such as the change in the morphology of the samples and the release of gases over a wider temperature range, which can lead to the preferential formation of micropores over mesopores when low quantities of biuret are added.

It is hypothesised that the porosity of the samples is created through the release of gases during the decomposition of the chemicals. Therefore, the variation in porosity is assigned to the differences in decomposition temperatures and pathways of the various precursors. Biuret decomposes at a slighly higher temperature than urea (190 °C *versus* 150 °C), and exhibits a similar two-step decomposition pattern to that of urea (**Fig. S5a**). On the other hand, melamine decomposes in a single step (~260 °C). To understand the formation of porous BN using different precursors, mixtures of boric acid and urea, as well as boric acid, urea and biuret were analysed *via* thermogravimetry (**Fig. S5b**). The decomposition profile varies significantly between the different mixtures, with a wider range of decomposition temperature for the multiple N-precursor mixture (**Fig. S5b**). Hence, it is envisioned that for the multiple N-precursor BN samples, urea starts decomposing at a lower temperature, thereby releasing gases, such as ammonia, that react with boric acid/boron oxide to form BN. Both biuret and melamine decompose at higher temperatures, meaning gases are released over a wider range of temperatures compared to the use of a single N-precursor. These gases act as porogens for boron nitride. While this hypothesis is proposed, one could argue that the increase in surface area

observed derives from the increase in N/B molar ratio, as previously reported from Nag *et al.* [12] for urea and boric acid precursors. However, the highest surface area samples exhibit N:B molar ratios of 16 and 22. When similar ratios were used to produce single N-precursor BN samples, surface areas of ~900 m^2/g were measured, compared to more than 1500 m^2/g for multiple N-precursor BN samples. This points to the fact that the use of multiple N-precursors with a wide thermal decomposition range is indeed fundamental in enhancing the surface area of the material.

As surface chemistry is also critically important when gas sorption applications are considered, the chemical features of the materials were analysed. All samples exhibit the two characteristic IR bands of h-BN (1350 cm^{-1}: B-N in-plane stretching mode; 800 cm^{-1}: B-N-B out-of-plane bending; **Fig. S6**).[45] The samples were further analyzed using XPS (**Fig. S7**). The analysis of the core level spectra for B 1*s* and N 1*s* confirms the formation of BN from the peaks at 191.0 eV and 398.6 eV, respectively. The presence of satellite peaks, which are typical for the hexagonal form of BN, are observed at higher binding energies.[46-48] The presence of such peaks suggests that the samples contain some hexagonal phase, despite them being almost entirely amorphous. This supports the observations made earlier based on TEM analysis (**Fig. 1**). The samples exhibit oxygen, as observed in other studies,[40] attributed to a boronoxynitride compound. The variation in oxygen content is likely associated with the preparation of the samples, such as time between the degas and the start of the XPS analysis. Hence, the oxygen species must have been primarily located at the surface of the samples. The amount of carbon impurities is low. Carbon species are mostly belonging to adventitious carbon.

Owing to their high porosity and due to the presence of N atoms, the materials were studied for CO_2/N_2 separation (at both low and high pressures) and CO_2/CH_4 separation, two separations that are directly relevant to the energy sector in the context of carbon capture and natural gas

processing, respectively. As expected, the results point to the positive impact of the (micro)porosity enhancement on the CO_2 sorption capacity (**Fig. S8**, **Fig. S9**). At 1 bar, porous BN adsorbs up to 1.6 mmol/g of CO_2, which is approximately four times higher than the best performing porous BN material tested thus far under the same conditions (**Fig. S8a**).[13] Nevetherless, it is noted that the sorption capacity of BN remains limited if compared to other classes of porous materials.[49,50] This is due to the fact that at low pressure, chemisorption is the key mechanism. Considering the high micropore volume of the porous BN samples, it was hypothesised that these could be better suited for high pressure applications. For this reason, the highest surface area BN sample was tested for CO_2 sorption at high pressure (up to 20 bar) and various temperatures (10, 25 and 40 °C, **Fig. S8b**). The CO_2 sorption capacity measured at 25 °C and 20 bar (8.3 mmol/g) is higher than that reported for commerial zeolites and comparable to that reported for commercial activated carbon under similar conditions.[51] When considering CO_2 capture, BN has the advantage of not being affected by the presence of moisture as opposed to zeolites and certain types of MOFs, and it is more chemically resistant than activated carbon. The heat of adsorption for CO_2 is approximately 19 kJ/mol (**Fig. S8**). This value is aligned with theoretical calculation for CO_2 physisorption on a BN sheet.[52]

Powders are not suitable for use at an industrial scale and eventually adsorbents must be structured in order to minimise pressure drop. Pelletizing is commonly conducted to address this aspect but is also known to lower the porosity and, therefore, the overall capacity. This loss in porosity is due to either the 'collapse' of pores due to the formation of pellets and/or the addition of a binder (*i.e.* an 'inactive' component), reducing the gravimetric and volumetric uptakes. Porous BN pellets obtained from BN-MU1:5 samples (sample derived from melamine and urea) were prepared (**Fig. 4a**) and their porosity was analysed using N_2 sorption isotherms (**Fig. 4a)**.

The isotherms exhibit a similar shape to that of the non-pelletized BN and a limited decrease in the surface area and volume of pores is observed (average decrease over four repeats: 16 % for surface area, 19 % for total pore volume and 17 % for micropore volume). This shows that most of the original pore structure is maintained after compression and highlights the great mechanical stability and processability of porous BN powder. Interestingly, CO_2 sorption capacity of a BN pellet at 25 °C is 1.1 mmol/g at 1 bar (1.6 mmol/g for non-pelletized sample) and roughly 8.4 mmol/g ± 2 % at 20 bar (8.3 mmol/g ± 2 % for non-pelletized sample) (**Fig. 4b**). A hypothesis - not confirmed at this stage - for the absence of a decreased CO_2 capacity is the fact that pelletizing introduces defects in the material structure (*e.g.* dangling bonds), which subsequently favour adsorption.

CONCLUSIONS

A facile template-free synthesis is formulated for the production of highly porous BN, whose pore network is directly visualized using tomography and fully characterized from the nano- to the macro-scale using a range of analytical tools. The synthesis involves fewer steps and cheaper chemicals when compared to other methods, while maintaining, and in some cases surpassing, the porosity of the materials reported to date. A key aspect of our approach is that it enables the tunability of not only the total porosity, but also the microporosity. The method relies on the use of multiple N-containing precursors, whose thermal decompositions span a large temperature range and enables the progressive release of porogens as BN formation takes place. The most porous samples exhibit enhanced CO_2 capture capacity compared to commercial zeolites at high pressure and can be shaped as pellets with little or no reduction in porosity and gas uptake.

METHODS

Material synthesis

Porous BN was synthesized starting from different nitrogen-containing precursors and boric acid. The N-precursors used were urea (molecular biology grade, Sigma-Aldrich), melamine (melamine 99 %, Sigma-Aldrich) and biuret (biuret, Sigma-Aldrich). The B-precursor used was boric acid (ACS reagent, Sigma-Aldrich). In the following, when only one N-precursor was used, the samples are called "single N-precursor BN", while when two different N-precursors were used the samples are referred to as "multiple N-precursors BN".

Preparation of the reaction intermediates for the synthesis of single N-precursor BN

The intermediates consisted of either a mixture of urea and boric acid, a mixture of biuret and boric acid, or a mixture of melamine and boric acid. In the first two cases, the chemicals were physically mixed and ground. In the latter case, boric acid was first dissolved in an aqueous melamine solution before the water was completely evaporated to obtain a white precipitate, which was further dried overnight at 85 ºC. The molecular ratios urea:boric acid, biuret:boric acid and melamine:boric acid were equal to 5, 2 and 0.5, respectively. These were selected as they enabled the production of porous BN while obtaining a good product yield and/or minimizing the amount of impurities.[12, 14, 53,54]

Preparation of the reaction intermediates for the synthesis of multiple N-precursors BN

Here, biuret or melamine was used as N-precursor together with urea. Biuret and melamine acted as secondary N-precursors and were selected because they are relatively cheap, readily available, they decompose at higher temperatures compared to urea and they do not call for a post-synthesis cleaning step (*i.e.* precursors decompose in the form of gases and the remaining solids are part of the BN structure). In a typical synthesis, varying amounts of either biuret or melamine were added to a urea- and boric acid mixture. The molar ratio of urea to boric acid was

kept constant at 5, while the biuret to boric acid molar ratio ranged from 0.5 to 8 and that of melamine to boric acid ranged from 0.25 to 1. Prior to the synthesis of BN, all the precursors were physically mixed and ground. It must be noted that the molar ratio of melamine to boric acid was not increased over 1 as an excess of melamine leads to the formation of a sample with a large amount of carbon impurities.

Synthesis of porous BN using single or multiple N-precursors

The intermediates were placed in an alumina boat crucible and heated up to 1050 °C (10 °C/min ramp rate) under nitrogen gas flow (0.05 L/min during analysis, 2 h at 0.25 L/min to purge). The temperature was held at 1050 °C for 3.5 hours and the furnace was then allowed to cool naturally under a nitrogen atmosphere. A white powder was collected after the synthesis. Two different naming systems were used, depending on whether one or two N-precursor/s was/were used. The generic names are BN-A-X and BN-AC-X:Y, respectively. A and AC correspond to the N-precursors used: urea, biuret or melamine (A or C = U, B, M). X and Y correspond to the molar ratios of N-precursor to boric acid. For instance, BN-U5 indicates a sample prepared from a single N-precursor using a mixture of urea and boric acid in molar ratio of 5. BN-BU0.5:5 indicates a sample prepared from multiple N-precursors using a mixture of biuret:urea:boric acid in molar ratios 0.5:5:1.

Formation of pellets

Porous BN powder (BN-MU1:5, ~ 200 mg) was coarsely ground with an agate pestle and mortar and was placed into a pellet die (Specac, 13 mm evacuable stainless steel). The die was positioned into a manual press and 5 tonnes of load were applied to form a pellet. The pellet was carefully removed from the pelletizer through inverting the die and gradually applying a small load on its base.

Materials characterization

Structural properties and morphology: Powder X-ray diffraction (XRD) was performed using an X-ray diffractometer (PANalytical X'Pert PRO) in reflection mode. The operating conditions included an anode voltage of 40 kV and an emission current of 40 mA using monochromatic Cu Kα radiation (λ = 1.54178 Å). Nitrogen isotherms were measured using a porosity analyser (Micromeritics 3Flex) at -196 °C. Prior to the measurement, the samples were degassed overnight at 120 °C at roughly 0.2 mbar pressure. They were finally degassed *in-situ* on the porosity analyser for 4 hours down to around 0.0030 mbar. It must be noted that when BN was produced in the form of a pellet, this had to be fragmented in order to fit into the tubes used for nitrogen sorption analysis. The surface areas of the samples were calculated using the Brunauer-Emmett-Teller (BET) method.[55]The total volume of pores was calculated from the volume of N_2 adsorbed at $P/P_0 = 0.97$. The micropore volume was determined using the Dubinin Radushkevich method.[56] The pore size distribution was derived from the isotherms by using an in-built software from Micromeritics and selecting the DFT model for carbon slit shape pores (N2@77 on Carbon Slit Pores by NLDFT). The morphology of the samples was evaluated using a Scanning Electron Microscope (SEM, Leo Gemini 1525, Zeiss) in secondary electron mode (InLens detector) at 5 kV. The samples were ground, deposited on carbon tape and coated with 20 nm of chromium to reduce charging in the microscope. Transmission electron microscopy (TEM) imaging and FFT's diffraction patterns (for Figure 1) were collected on a JEOL 2100FX microscope. TEM and Scanning TEM (STEM) imaging were carried out on an FEI Titan 80-300 Cs image-corrected microscope, operated at 80kV and 300kV. Sample preparation was performed by dispersing porous BN powder in ethanol and drop-depositing the supernatant on a

holey carbon copper grid. STEM images were acquired using a convergence semi-angle of 10 mrad and an inner and outer collection angle to the high angle annular dark field (HAADF) detector of 40 and 196 mrad respectively. The bright contrast in the STEM images is from regions containing higher atomic number and/or density. For the tomograms, STEM images were acquired every 2° from -54 and +74° (for Figure 3E) and between -70 and +74° (for Figure 3B). The images were aligned and reconstructed using Inspect3D (FEI Visualization Group). A total of 64 and 62 images were used in each of the final reconstructions, respectively. The initial reconstruction was carried out using a weighted back projection (WBP) algorithm and then reconstructed using 25 iterations of a simultaneous iterative reconstruction technique (SIRT) algorithm. The reconstructed 3D TEM tomography data set was imported into Avizo (FEI Visualization Group, France) as a .rec file and more details on the steps of the reconstruction are provided in the Supporting Information.

Chemical properties: The thermal stability of the precursors was analyzed using a thermogravimetrical analyzer (TGA) Netzsch TG209 F1 Libra from ambient temperature to 900 °C (10 °C/min ramp rate) under nitrogen gas flow (0.1 L/min). The porous BN samples were characterized by Fourier Transform Infrared (FT-IR) spectroscopy. The samples were first ground in an agate mortar and spectra were collected in the range of 600-4000 cm^{-1} using a Perkin-Elmer Spectrum 100 Spectrometer equipped with an attenuated total reflectance (ATR) accessory. X-Ray Photoelectron Spectroscopy (XPS) was performed using a Thermo Scientific K-Alpha^{+} X-ray Photoelectron Spectrometer equipped with a MXR3 Al Kα monochromated X-ray source (hν = 1486.6 eV). X-ray gun power was set to 72 W (6 mA and 12 kV). All high resolution spectra (B 1*s*, N 1*s*, C 1*s*, and O 1*s*) were acquired using 20 eV pass energy and 0.1 eV step size. The samples were ground and mounted on the XPS sample holder using

conductive carbon tape. Thermo Avantage software (ThermoFisher Scientific) was used to analyse the data. The XPS spectra were shifted to align the peak for adventitious carbon (C-C) at 285.0 eV.

Gas sorption

Low pressure: Gas sorption tests at low pressure (up to 1 bar) were performed on a Micromeritics 3Flex sorption analyzer at 25 °C, using a water bath to control the temperature. The samples (~ 100 mg) were degassed overnight at 120 °C at roughly 0.2 mbar pressure and further degassed *in-situ* for 4 hours down to around 0.0030 mbar, before the start of the analysis. The gases were tested in the following order: nitrogen, methane, carbon dioxide; and the *in-situ* degas step was repeated between each measurement.

High pressure: Gas sorption tests at high pressures (up to 20 bar) were performed gravimetrically on an Intelligent Gas Analyzer IGA-200 from Hiden Isochema. The sample (~ 30 mg) was added to a porous sample container, connected to a high-precision balance (± 0.0001 mg). The sample was degassed *in-situ* at 120 ºC, using a furnace attachment, for 4 hours before the start of the analysis. Ultra-high vacuum of up to 10^{-6} mbar can be created inside the chamber. Nitrogen and carbon dioxide sorption were performed at different temperatures (10, 25, 40 °C) and the sample was degassed at 60 °C for 3 h between each run. The temperature was controlled by using a water/ethylene glycol bath.

Calculation of the heat of adsorption and entropy for CO_2

The heat of adsorption (Q_{st}) and entropy (ΔS) for CO_2 were calculated by fitting the gas sorption isotherms, collected at 3 different temperatures, with a Langmuir-Freudlich equation[57] (1):

$$y = \frac{abx^{1-c}}{1 + bx^{1-c}} \qquad (1)$$

The fitting was used to calculate the pressures (P) at desired CO_2 loadings (0.1-5). ln(P) was then plotted against $\frac{1}{T}$ for each selected loading and fitted with a linear fit. Based on the Van't Hoff equation[58] the heat of adsorption and entropy were finally calculated from equations (2,3).

$$Q_{st} = -mR \qquad (2)$$

$$\Delta S = -cR \qquad (3)$$

Where m is the slope, c is the intercept and R is the universal gas constant.

ACKNOWLEDGMENTS

The authors would like to thank L. Bolton and P. Howard for their technical input, M. Abdulsalam Ebrahim and M. Cook for their help with the sorption analysis and C. Constantinou for his help in the synthesis. The authors would also like to acknowledge the funding and technical support from BP through the BP International Centre for Advanced Materials (BP-ICAM), which made this research possible as well as EPSRC for the funding through the CDT in Advanced Characterization of Materials (CDT-ACM) (EP/L015277/1).

ASSOCIATED CONTENT

Supporting Information Available:

Experimental section with details on tomography reconstruction, structural parameters derived from N_2 sorption isotherms at -196 °C for all BN samples (**Table S1**), XRD patterns for porous BN samples (**Fig. S1**), SEM images for porous BN samples (**Fig. S2**), TEM images for BN-U5

and BN-MU1:5 (**Fig. S3**), pore size distribution for porous BN samples (**Fig. S4**), TGA curves with thermal decomposition of precursors and mixtures of precursors (**Fig. S5**), FTIR spectra for porous BN samples (**Fig. S6**), XPS N 1*s*, B 1*s* and O 1*s* core level spectra for porous BN samples (**Fig. S7**), high pressure CO_2 and N_2 sorption for BN powder at different temperatures; low pressure CO_2, N_2 and CH_4 sorption for BN powder and heat of adsorption for CO_2 for BN powder (**Fig. S8**) bar plots with CO_2, N_2 and NH_4 sorption capacities for porous BN samples tested at 25 °C and 1 bar (**Fig. S9**), Videos displaying the images aligned collected with TEM tomography for a single N-precursor BN-U5 (**Movie 1**) and a multiple N-precursor BN-MU1:5 (**Movie 2)**.

This material is available free of charge *via* the Internet at http://pubs.acs.org.

AUTHOR INFORMATION

Corresponding Author

*Camille Petit, camille.petit@imperial.ac.uk

The authors declare no competing financial interest.

REFERENCES

1. Parlett, C. M.; Wilson, K.; Lee, A. F., Hierarchical Porous Materials: Catalytic Applications. *Chem. Soc. Rev.* **2013,** *42*, 3876-3893.
2. Weng, Q.; Wang, B.; Wang, X.; Hanagata, N.; Li, X.; Liu, D.; Wang, X.; Jiang, X.; Bando, Y.; Golberg, D., Highly Water-Soluble, Porous, and Biocompatible Boron Nitrides for Anticancer Drug Delivery. *ACS Nano* **2014,** *8*, 6123-6130.
3. Adebajo, M. O.; Frost, R. L.; Kloprogge, J. T.; Carmody, O.; Kokot, S., Porous Materials for Oil Spill Cleanup: a Review of Synthesis and Absorbing Properties. *J. Porous Mater.* **2003,** *10*, 159-170.
4. Rouquerol, J.; Rouquerol, F.; Llewellyn, P.; Maurin, G.; Sing, K. S., *Adsorption by Powders and Porous Solids: Principles, Methodology and Applications*. Academic press: 2013.
5. Wang, S.; Peng, Y., Natural Zeolites As Effective Adsorbents in Water and Wastewater Treatment. *Chem. Eng. J.* **2010,** *156*, 11-24.
6. Yin, C. Y.; Aroua, M. K.; Daud, W. M. A. W., Review of Modifications of Activated Carbon for Enhancing Contaminant Uptakes from Aqueous Solutions. *Sep. Purif. Technol.* **2007,** *52*, 403-415.
7. Shafeeyan, M. S.; Daud, W. M. A. W.; Houshmand, A.; Shamiri, A., A Review on Surface Modification of Activated Carbon for Carbon Dioxide Adsorption. *J. Anal. Appl. Pyrolysis* **2010,** *89*, 143-151.
8. Lee, J.; Farha, O. K.; Roberts, J.; Scheidt, K. A.; Nguyen, S. T.; Hupp, J. T., Metal–Organic Framework Materials As Catalysts. *Chemical Society Reviews* **2009,** *38*, 1450-1459.
9. Ding, S.-Y.; Wang, W., Covalent Organic Frameworks (COFs): From Design to Applications. *Chem. Soc. Rev.* **2013,** *42*, 548-568.
10. Lu, X.; Jin, D.; Wei, S.; Wang, Z.; An, C.; Guo, W., Strategies to Enhance CO_2 Capture and Separation Based on Engineering Absorbent Materials. *J. Mater. Chem. A* **2015,** *3*, 12118-12132.
11. Janik, J. F.; Ackerman, W. C.; Paine, R. T.; Hua, D.-W.; Maskara, A.; Smith, D. M., Boron Nitride As a Selective Gas Adsorbent. *Langmuir* **1994,** *10*, 514-518.
12. Nag, A.; Raidongia, K.; Hembram, K. P.; Datta, R.; Waghmare, U. V.; Rao, C., Graphene Analogues of BN: Novel Synthesis and Properties. *ACS Nano* **2010,** *4*, 1539-1544.
13. Xiao, F.; Chen, Z.; Casillas, G.; Richardson, C.; Li, H.; Huang, Z., Controllable Synthesis of Few-layered and Hierarchically Porous Boron Nitride Nanosheets. *Chem. Commun.* **2016,** *52*, 3911-3914.
14. Li, J.; Lin, J.; Xu, X.; Zhang, X.; Xue, Y.; Mi, J.; Mo, Z.; Fan, Y.; Hu, L.; Yang, X., Porous Boron Nitride with a High Surface Area: Hydrogen Storage and Water Treatment. *Nanotechnology* **2013,** *24*, 155603-155609.
15. Weng, Q.; Wang, X.; Zhi, C.; Bando, Y.; Golberg, D., Boron Nitride Porous Microbelts for Hydrogen Storage. *ACS Nano* **2013,** *7*, 1558-1565.
16. Lei, W.; Zhang, H.; Wu, Y.; Zhang, B.; Liu, D.; Qin, S.; Liu, Z.; Liu, L.; Ma, Y.; Chen, Y., Oxygen-Doped Boron Nitride Nanosheets with Excellent Performance in Hydrogen Storage. *Nano Energy* **2014,** *6*, 219-224.
17. Maleki, M.; Beitollahi, A.; Shokouhimehr, M., Simple Synthesis of Two-Dimensional Micro/Mesoporous Boron Nitride. *Eur. J. Inorg. Chem.* **2015**, *14,* 2478-2485.

18. Weng, Q.; Wang, X.; Bando, Y.; Golberg, D., One-Step Template-Free Synthesis of Highly Porous Boron Nitride Microsponges for Hydrogen Storage. *Adv. Energy Mater.* **2014,** *4*,1301525-1301532.
19. Lian, G.; Zhang, X.; Zhang, S.; Liu, D.; Cui, D.; Wang, Q., Controlled Fabrication of Ultrathin-Shell BN Hollow Spheres with Excellent Performance in Hydrogen Storage and Wastewater Treatment. *Energy Environ. Sci.* **2012,** *5*, 7072-7080.
20. Grant, J.; Carrero, C.; Goeltl, F.; Venegas, J.; Mueller, P.; Burt, S.; Specht, S.; McDermott, W.; Chieregato, A.; Hermans, I., Selective Oxidative Dehydrogenation of Propane to Propene Using Boron Nitride Catalysts. *Science* **2016,** *354*, 1570-1573.
21. Venegas, J. M.; Grant, J. T.; McDermott, W. P.; Burt, S. P.; Micka, J.; Carrero, C. A.; Hermans, I., Selective Oxidation of n-Butane and Isobutane Catalyzed by Boron Nitride. *ChemCatChem* **2017,** *9,* 1-11.
22. Economy, J.; Anderson, R. Boron Nitride Fibers, *J. Polym. Sci., Part C: Polym. Lett.,***1967**, 19,283-297.
23. Eichler, J.; Lesniak, C., Boron Nitride (BN) and BN Composites for High-Temperature Applications. *J. Eur. Ceram. Soc.* **2008,** *28*, 1105-1109.
24. Chen, Y.; Zou, J.; Campbell, S. J.; Le Caer, G., Boron Nitride Nanotubes: Pronounced Resistance to Oxidation. *Appl. Phys. Lett.* **2004,** *84*, 2430-2432.
25. Lipp, A.; Schwetz, K. A.; Hunold, K., Hexagonal Boron Nitride: Fabrication, Properties and Applications. *J. Eur. Ceram. Soc.* **1989,** *5*, 3-9.
26. Lavrenko, V.; Alexeev, A., High-temperature oxidation of Boron Nitride. *Ceram. Int.* **1986,** *12*, 25-31.
27. Corrigan, F.; Bundy, F., Direct Transitions Among the Allotropic Forms of Boron Nitride at High Pressures and Temperatures. *J. Chem. Phys.* **1975,** *63*, 3812-3820.
28. Dibandjo, P.; Chassagneux, F.; Bois, L.; Sigala, C.; Miele, P., Comparison Between SBA-15 Silica and CMK-3 Carbon Nanocasting for Mesoporous Boron Nitride Synthesis. *J. Mater. Chem.* **2005,** *15*, 1917-1923.
29. Rushton, B.; Mokaya, R., Mesoporous Boron Nitride and Boron-Nitride-Carbon Materials from Mesoporous Silica Templates. *J. Mater. Chem.* **2008,** *18*, 235-241.
30. Schlienger, S.; Alauzun, J.; Michaux, F.; Vidal, L.; Parmentier, J.; Gervais, C.; Babonneau, F.; Bernard, S.; Miele, P.; Parra, J., Micro-, Mesoporous Boron Nitride-Based Materials Templated from Zeolites. *Chem. Mater.* **2011,** *24*, 88-96.
31. Han, W.-Q.; Brutchey, R.; Tilley, T. D.; Zettl, A., Activated Boron Nitride Derived from Activated Carbon. *Nano Letters* **2004,** *4*, 173-176.
32. Alauzun, J. G.; Ungureanu, S.; Brun, N.; Bernard, S.; Miele, P.; Backov, R.; Sanchez, C., Novel Monolith-Type Boron Nitride Hierarchical Foams Obtained Through Integrative Chemistry. *J. Mater. Chem.* **2011,** *21*, 14025-14030.
33. Dibandjo, P.; Bois, L.; Chassagneux, F.; Cornu, D.; Letoffe, J. M.; Toury, B.; Babonneau, F.; Miele, P., Synthesis of Boron Nitride with Ordered Mesostructure. *Adv.Mater.* **2005,** *17*, 571-574.
34. Vinu, A.; Terrones, M.; Golberg, D.; Hishita, S.; Ariga, K.; Mori, T., Synthesis of Mesoporous BN and BCN Exhibiting Large Surface Areas *via* Templating Methods. *Chem. Mater.* **2005,** *17*, 5887-5890.
35. Suryavanshi, U.; Balasubramanian, V. V.; Lakhi, K. S.; Mane, G. P.; Ariga, K.; Choy, J.-H.; Park, D.-H.; Al-Enizi, A. M.; Vinu, A., Mesoporous BN and BCN Nanocages with High Surface Area and Spherical Morphology. *Phys. Chem. Chem. Phys.* **2014,** *16*, 23554-23557.

36. Dibandjo, P.; Bois, L.; Chassagneux, F.; Miele, P., Thermal Stability of Mesoporous Boron Nitride Templated with a Cationic Surfactant. *J. Eur. Ceram. Soc.* **2007,** *27*, 313-317.
37. Li, J.; Xiao, X.; Xu, X.; Lin, J.; Huang, Y.; Xue, Y.; Jin, P.; Zou, J.; Tang, C., Activated Boron Nitride As an Effective Adsorbent for Metal Ions and Organic Pollutants. *Sci. Rep.* **2013,** *3,* 3208-3214.
38. Lei, W.; Portehault, D.; Liu, D.; Qin, S.; Chen, Y., Porous Boron Nitride Nanosheets for Effective Water Cleaning. *Nat. Commun* **2013,** *4*, 1777-1783.
39. Wu, P.; Zhu, W.; Chao, Y.; Zhang, J.; Zhang, P.; Zhu, H.; Li, C.; Chen, Z.; Li, H.; Dai, S., A Template-Free Solvent-Mediated Synthesis of High Surface Area Boron Nitride Nanosheets for Aerobic Oxidative Desulfurization. *Chem. Commun.* **2016,** *52*, 144-147.
40. Marchesini, S.; Regoutz, A.; Payne, D.; Petit, C., Tunable Porous Boron Nitride: Investigating its Formation and its Application for Gas Adsorption. *Microporous Mesoporous Mater.* **2017,** *243*, 154-163.
41. Kurakevych, O. O.; Solozhenko, V. L., Rhombohedral Boron Subnitride, B13N2, by X-ray Powder Diffraction. *Acta Crystallogr., Sect. C: Cryst. Struct. Commun* **2007,** *63*, i80-i82.
42. Hagio, T.; Nonaka, K.; Sato, T., Microstructural Development with Crystallization of Hexagonal Boron Nitride. *J. Mater. Sci. Lett.* **1997,** *16*, 795-798.
43. Zhu, Y.; Murali, S.; Cai, W.; Li, X.; Suk, J. W.; Potts, J. R.; Ruoff, R. S., Graphene and Graphene Oxide: Synthesis, Properties, and Applications. *Adv. Mater.* **2010,** *22*, 3906-3924.
44. Li, J.; Xiao, X.; Xu, X.; Lin, J.; Huang, Y.; Xue, Y.; Jin, P.; Zou, J.; Tang, C., Activated Boron Nitride As an Effective Adsorbent for Metal Ions and Organic Pollutants. *Sci. Rep.* **2013,** *3*, 3208-3213.
45. Geick, R.; Perry, C.; Rupprecht, G., Normal Modes in Hexagonal Boron Nitride. *Phys. Rev.* **1966,** *146*, 543.
46. Nazarov, A. S.; Demin, V. N.; Grayfer, E. D.; Bulavchenko, A. I.; Arymbaeva, A. T.; Shin, H. J.; Choi, J. Y.; Fedorov, V. E., Functionalization and Dispersion of Hexagonal Boron Nitride (h-BN) Nanosheets Treated with Inorganic Reagents. *Chem. - Asian J.* **2012,** *7*, 554-560.
47. Park, K.; Lee, D.; Kim, K.; Moon, D., Observation of a Hexagonal BN Surface Layer on the Cubic BN Film Grown by Dual Ion Beam Sputter Deposition. *Appl. Phys. Lett.* **1997,** *70*, 315-317.
48. Riviere, J.; Pacaud, Y.; Cahoreau, M., Spectroscopic Studies of BN Films Deposited by Dynamic Ion Mixing. *Thin Solid Films* **1993,** *227*, 44-53.
49. Aijaz, A.; Fujiwara, N.; Xu, Q., From Metal–Organic Framework to Nitrogen-Decorated Nanoporous Carbons: High CO_2 Uptake and Efficient Catalytic Oxygen Reduction. *J. Am. Chem. Soc.* **2014,** *136*, 6790-6793.
50. Li, J.-R.; Kuppler, R. J.; Zhou, H.-C., Selective Gas Adsorption and Separation in Metal–Organic Frameworks. *Chem. Soc. Rev.* **2009,** *38*, 1477-1504.
51. Millward, A. R.; Yaghi, O. M., Metal-Organic Frameworks with Exceptionally High Capacity for Storage of Carbon Dioxide at Room Temperature. *J. Am. Chem. Soc.* **2005,** *127*, 17998-17999.
52. Sun, Q.; Li, Z.; Searles, D. J.; Chen, Y.; Lu, G.; Du, A., Charge-Controlled Switchable CO_2 Capture on Boron Nitride Nanomaterials. *J. Am. Chem.Soc.* **2013,** *135*, 8246-8253.
53. Roy, A.; Choudhury, A.; Rao, C. N. R., Supramolecular Hydrogen-Bonded Structure of a 1: 2 Adduct of Melamine with Boric Acid. *J. Mol. Struct.* **2002,** *613*, 61-66.
54. Hubáček, M.; Sato, T.; Ishii, T., A Coexistence of Boron Nitride and Boric Oxide. *J. Solid State Chem.* **1994,** *109*, 384-390.

55. Brunauer, S.; Emmett, P. H.; Teller, E., Adsorption of Gases in Multimolecular Layers. *J. Am. Chem. Soc.* **1938,** *60*, 309-319.
56. Chen, S.; Yang, R., Theoretical Basis for the Potential Theory Adsorption Isotherms. The Dubinin-Radushkevich and Dubinin-Astakhov Equations. *Langmuir* **1994,** *10*, 4244-4249.
57. Umpleby, R. J.; Baxter, S. C.; Chen, Y.; Shah, R. N.; Shimizu, K. D., Characterization of Molecularly Imprinted Polymers with the Langmuir− Freundlich Isotherm. *Anal. Chem.* **2001,** *73*, 4584-4591.
58. Chaires, J. B., Possible Origin of Differences Between Van't Hoff and Calorimetric Enthalpy Estimates. *Biophys. Chem.* **1997,** *64*, 15-23.

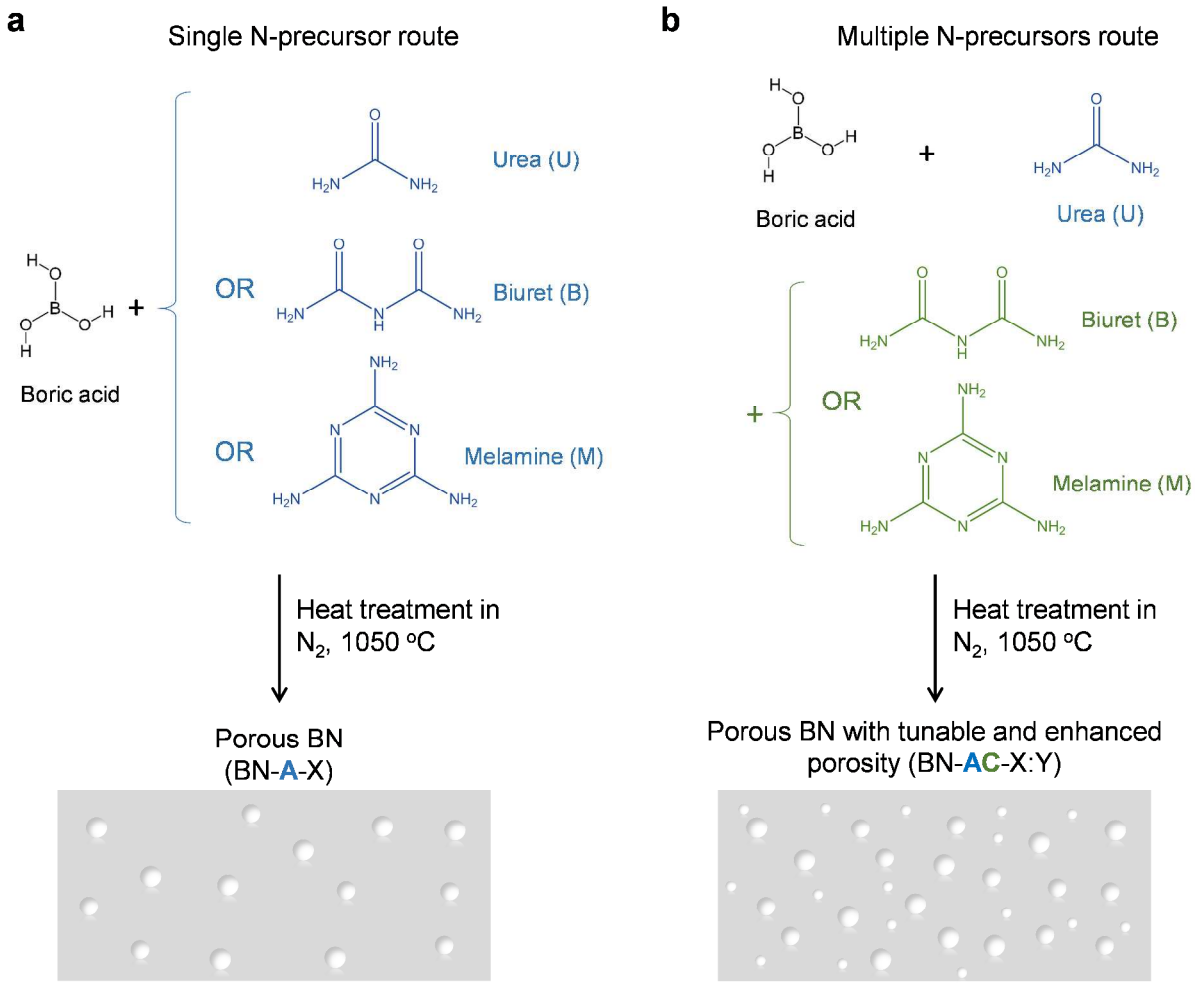

Scheme 1. Template-free synthesis methods for porous boron nitride using: (**a)** a single N-containing precursor route; (**b)** a two N-containing precursors route. All samples have been prepared *via* a gas-solid reaction under a flow of N_2. The generic names for the samples are BN-A-X and BN-AC-X:Y, respectively. A and AC correspond to the N-precursors used: urea, biuret or melamine (A or C = U, B, M). X and Y correspond to the molar ratios of N-containing precursor to boric acid.

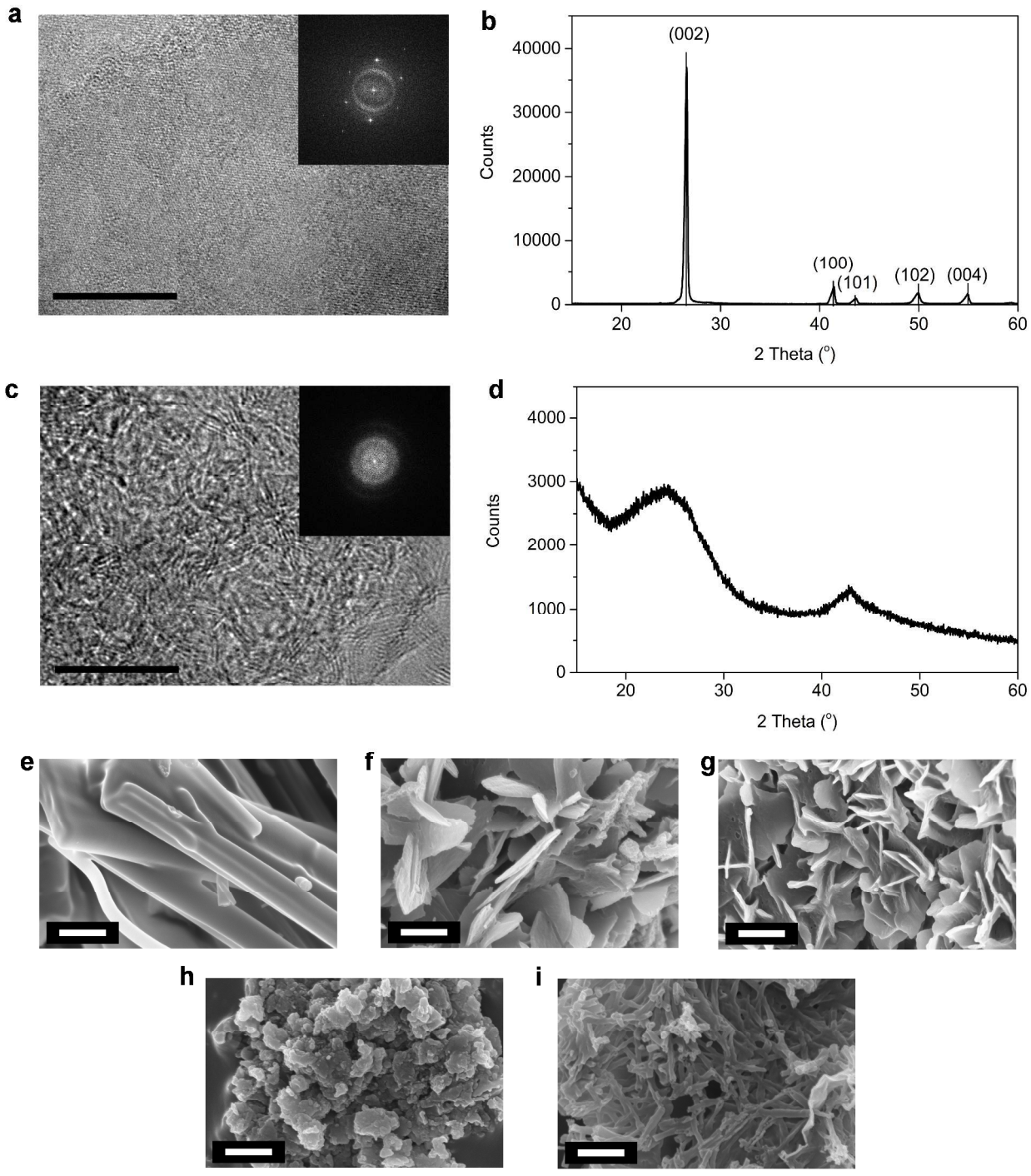

Figure 1. Morphology of the synthesized porous boron nitride. **(a**, **c)** Typical high resolution TEM images with FFT's diffraction patterns for: (**a)**, exfoliated h-BN exhibiting the expected crystalline pattern and **c**, porous BN (BN-U5 sample) exhibiting a disordered structure with some

crystalline regions. Scale bars in Figures (**a)** and (**c)** are 10 nm. (**b**, **d**) Typical XRD patterns for: (**b)**, h-BN commercial powder confirming the crystalline nature of the material and (**d)**, porous BN (BN-U5 sample) pointing to the presence of a combined turbostratic and amorphous material. (**e-g)**, SEM images for single N-precursor BN ((**e)** BN-MU0.5, (**f)** BN-U5 and (**g**) BN-B2) showing different morphologies – from fibres to flakes – depending on the precursors. (**h**, **i**) SEM images of multiple N-precursor BN ((**h)** BN-MU1:5, (**i**) BN-BU4:5) indicating a greater disorder/finer structure compared to single N-precursor BN. Scale bars in Figures (**e-i)** are 800 nm.

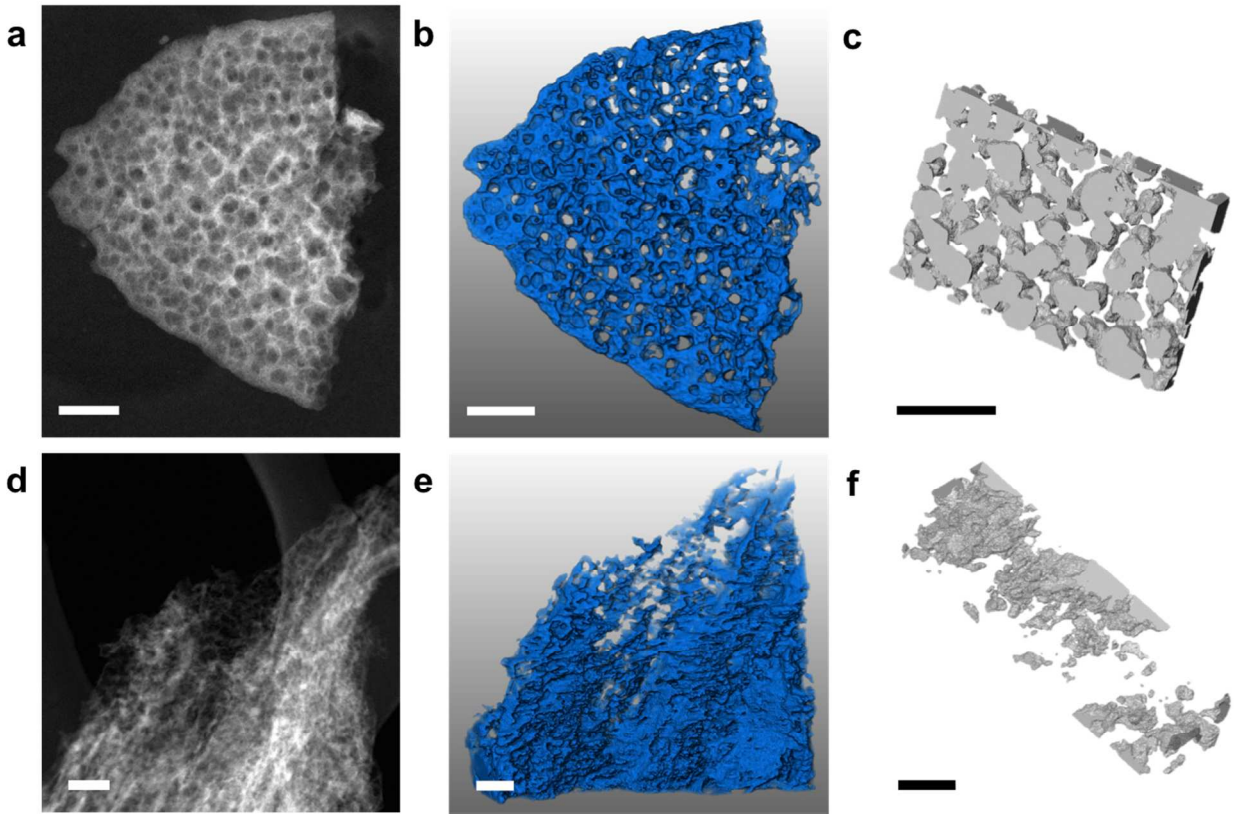

Figure 2. Mesoporosity of boron nitride. **(a**, **d**) Dark field STEM images of porous boron nitride samples synthized using: (**a)** a single N-precursor (*i.e.* urea, BN-U5 sample); (**d**) multiple N-precursor (*i.e.* urea and melamine, BN-MU1:5 sample). (**b, e**) 3D tomography reconstructions of the 2 samples; (**c, f)** 3D reconstructions of the pores. The scale bars represent 100 nm. These images reveal the distinct mesoporous networks of the two types of porous BN samples. The single N-precursor BN appears as a micro-sponge while the multiple N-precursor BN exhibits finer and more inhomogeneous features.

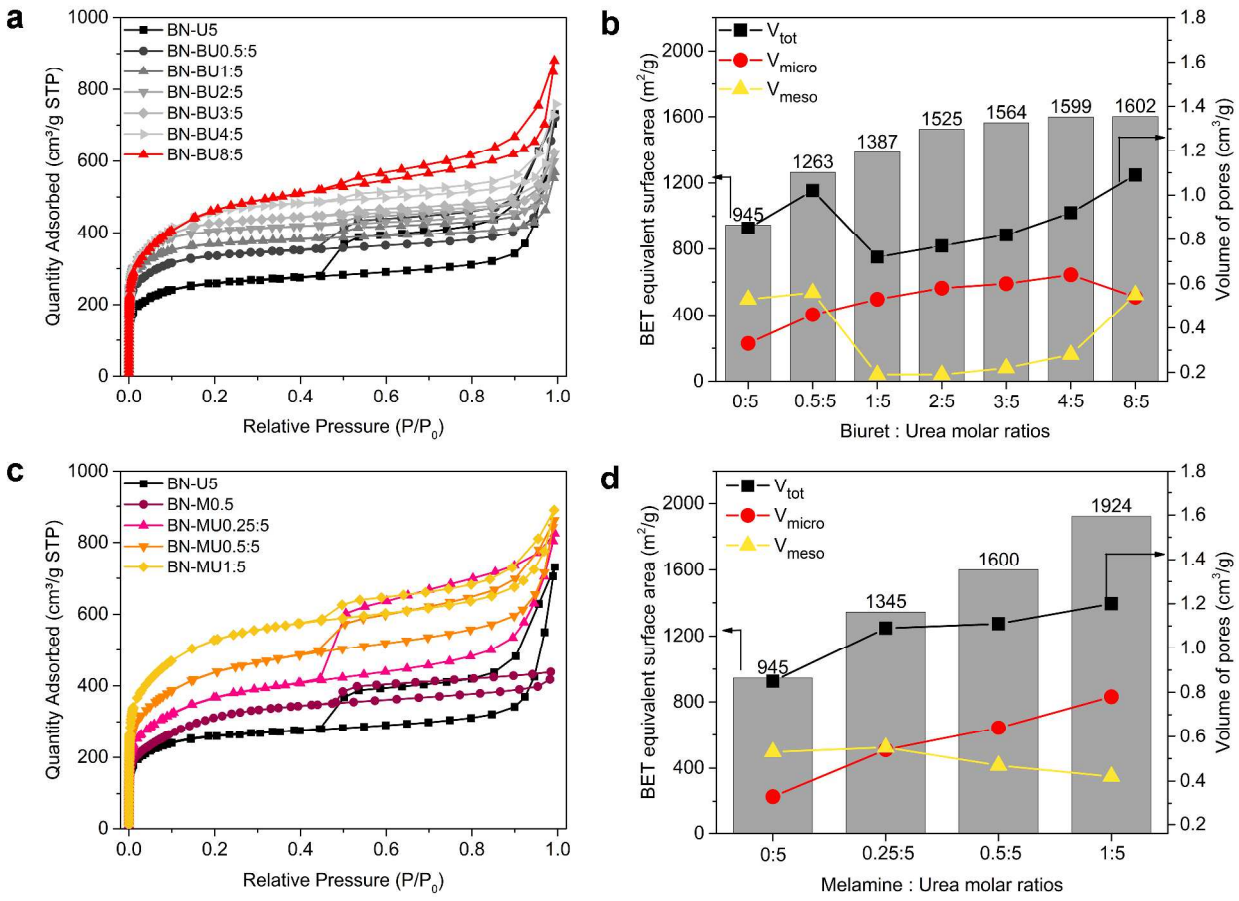

Figure 3. Tunable micro- and mesoporosity of boron nitride. (**a**, **c**) N_2 sorption isotherms measured at -196 °C for the BN samples synthesised from: (**a**) urea, biuret and boric acid mixtures and (**c**) urea, melamine and boric acid mixtures, all showing a gradual increase in the gas uptake and therefore porosity as more of the additional N-precursor is added. (**b**, **d**) Bar plots showing the BET equivalent surface areas, total volume of pores, micropore and mesopore volume for samples synthesised from: (**b**) urea, biuret and boric acid mixtures as well as (**d**) urea, melamine and boric acid mixtures, exhibiting a gradual microporosity enhancement as more of the additional N-precursor is added.

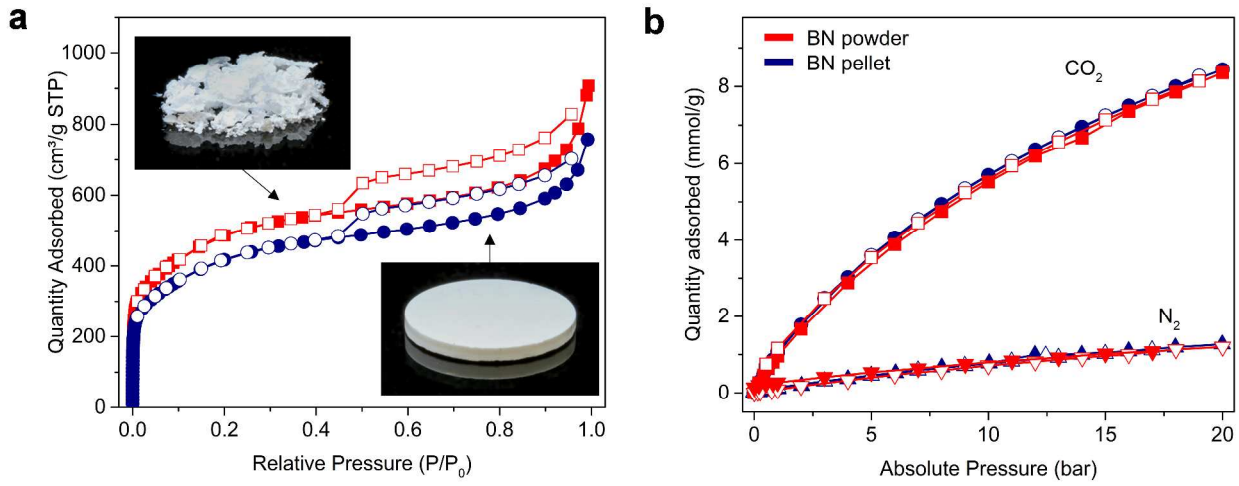

Figure 4. Gas uptake properties of the synthesised porous boron nitride. (**a)** N_2 sorption isotherms at -196 °C of porous BN before and after pelletizing (performed using a manual press and a 5 tonnes load) with the corresponding photographs of the materials in powder and pellet forms. (**b**) CO_2 and N_2 sorption isotherms for a porous boron nitride (BN-MU1:5 sample) and the corresponding pellet at 25 °C and up to 20 bar, as measured using a gravimetric system. Minimal reduction in porosity and gas uptake is observed after pelletizing.

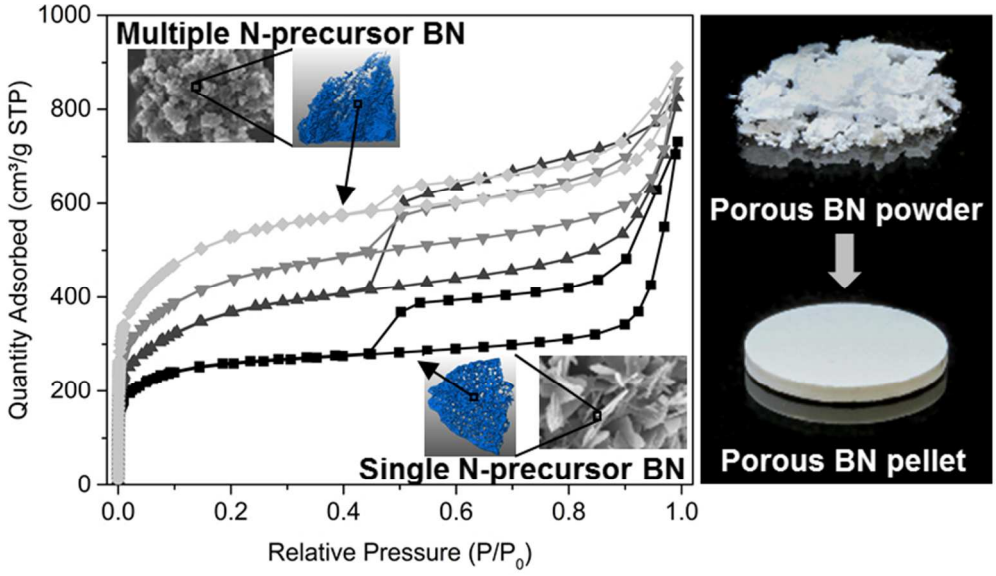

Table of Content

69x39mm (300 x 300 DPI)